ELSEVIER

Journal of Molecular Catalysis A: Chemical 167 (2001) 67–79

JOURNAL OF MOLECULAR CATALYSIS A: CHEMICAL

www.elsevier.com/locate/molcata

Low temperature FT-IR studies of NO adsorption on aluminum oxide and supported palladium

Dilip K. Paul*, Barry W. Smith[1], Chad D. Marten[2], Justin Burchett

Department of Chemistry, Pittsburg State University, Pittsburg, KS 66762, USA

Received 6 April 2000

Abstract

Low temperature FT-IR spectroscopy has been utilized to study the adsorption and thermal decomposition of NO on Al_2O_3 and Al_2O_3-supported palladium. At 110 K the nitric oxide adsorbs molecularly and reversibly via H-bonding to isolated surface –OH groups forming the $(NO)_2$ dimer. The dimer formation was characterized by symmetric and antisymmetric ν(N–O) stretching modes at 1871 and 1761 cm^{-1}, respectively. However, upon warming the adsorbed $(NO)_2$ dimer decomposes to form adsorbed nitrous oxide. The reactive species is thus shown to be the adsorbed dimer, which cannot be formed at temperatures greater than 140 K for lack of H-bonding. As the palladium loading is increased, there is a gradual decrease in $(NO)_2$ dimer formation with an increase in chemisorbed Pd–NO because of adsorption site transfer from Al_2O_3 to Pd.

Keywords: FT-IR studies; NO adsorption; Palladium; Aluminium oxide

1. Introduction

The adsorption and reactions of NO on various transition metal surfaces has received considerable attention. The catalytic reduction of NO plays an important role in the control of air pollution [1–3]. Since NO has an unpaired electron in the antibonding $2\pi^*$ orbital the adsorption and reactions of NO are not as well understood as those of CO. Dissociative as well as molecular adsorption of NO and combinations of both have been found.

Bertolo and coworkers [4,5] studied the NO adsorption on Pd(1 1 1) by means of HREELS, LEED, UPS, and $\Delta\Phi$ measurements in the temperature range between 20 and 100 K. At 20 K they noted the formation of the first layer of chemisorbed NO followed by a multilayer NO dimer formation as is concluded from the HREELS and UPS. Schmick and Wassmuth [6] also performed LEED, TDMS, and molecular beam measurements on the adsorption system NO/stepped Pd(1 1 1) down to 160 K. The saturation coverage at temperatures below 200 K is one monolayer, which is correlated with a sharp (2×2) LEED pattern. This pattern indicates that each molecule has two nearest neighbors at distances of 2.75 Å and two nearest neighbors at distances of 2.38 Å. These very small distances between neighboring NO molecules sug-

* Corresponding author. Tel.: +1-316-235-4872.
[1] Present address: Department of Chemistry, University of Wyoming, Laramie, WY 82701, USA.
[2] Present address: Department of Chemistry, Florida State University, Tallahassee, FL 32306, USA.

1381-1169/01/$ – see front matter
PII: S1381-1169(00)00492-1

gest the formation of NO dimers, in particular since the corresponding distance in solid dimerized NO is 2.40 Å. However, Goodman et al. [7] did not report any dimer formation on Pd(1 1 1) in the temperature range 120 and 250 K.

The formation of dimeric $(NO)_2$ was also reported for other metals such as Pt [8–10], Ag [11,12], and W [13] at very low temperatures. However, only the Ag(1 1 1) [12] and W [13] surfaces were found to be active to form N_2O upon low temperature adsorption of nitric oxide. Nitrous oxide formation for these two metals was believed to take place via an $(NO)_2$ dimer intermediate and the energy of activation for decomposition of the dimer was about 7.3 kJ mol^{-1} [12].

Early work on Y-type zeolites by Cho and Lunsford [14,15] suggested that NO dimerizes below 143 K which disproportionates to N_2O. A recent work on particulate of Cu on evaporated Al_2O_3 performed by Wu and Goodman [16] noticed the formation of N_2O. They explained that the formation of nitrous oxide was as a result of dissociative adsorption of NO at ∼110 K. Most recent studies on TiO_2 powders by Rusu and Yates [17] also suggested that the formation of N_2O at 118 K takes place through photolytic dissociative adsorption of NO.

The impetus behind this work has been the practical significance of Al_2O_3 as a catalyst and catalyst support. Typically, the Al_2O_3 surface is rich in a variety of structurally and chemically distinct hydroxyl groups [18–21] that condense together at high temperature to eliminate H_2O while yielding a coordinatively unsaturated Al^{3+} Lewis acid site and an oxide ion on the surface [18,19,22–25]. Strained Al–O–Al linkages, created during early stages of dehydroxylation, have been proposed to exist on the surface [22]; the identity of these sites has not been well established. Thus, the surface of Al_2O_3 provides a heterogeneous array of sites that enter into reaction with electron-donor and electron-acceptor molecules.

In this study, we present the results of a low temperature (below 300 K) infrared study of NO on high surface area Al_2O_3 and compare that to the interaction with Al_2O_3-supported Pd. These findings were then compared with other previous works on single crystal Pd surfaces in order to design a suitable metal catalyst. Nitric oxide adsorbs at low temperature via hydrogen bonding to the surface hydroxyl groups forming $(NO)_2$ dimer. Thermal decomposition at $T > 110$ K yields $(N_2O)_{ad}$ and formation of N_2O decreases as the Pd loading increases on the surface.

2. Experimental

2.1. Spectroscopic measurements and experimental apparatus

All transmission infrared spectra were measured using a purged Mattson RS-1 FT-IR spectrometer equipped with a narrow-band MCT detector. Spectra were recorded by coadding 500 scans at an instrument resolution of 4 cm^{-1} and signal gain of unity. Absorbance spectra reported represent single beam spectra ratioed to single beam spectra recorded for the freshly prepared sample (either Al_2O_3 or Pd/Al_2O_3 prior to reaction). Background sample spectra were collected at the same temperature before and after introduction of any gas so that the spectral change can be minimized by ratioing single beam spectra. Smoothing or background functions were not used during data handling and manipulation.

The stainless steel UHV infrared cell designed by Yates and coworkers [26] was used in these measurements. It consists of a main cell body (a double sided conflat flange) containing a CaF_2 disk that serves as the catalyst sample holder, held in place by a copper support ring which may be temperature controlled, using either cooled or heated N_2 (g). The cell body is mounted between two CaF_2 optical windows (Bicron Harshaw) sealed in standard 23/4 in. stainless steel conflat flanges. The IR cell is attached to a bakeable all metal gas-handling system and is typically maintained at a base pressure of 1×10^{-8} Torr by a 50 l/s turbomolecular pump. Rough pumping is achieved using a diaphragm pump. Sample temperatures were measured by a K-type thermocouple which is spot welded on the copper support ring. The studies by Yates [26] showed that the temperature difference between the copper support ring and the CaF_2 plate is within ±1 K throughout the temperature range of 83–300 K. The vacuum manifold is equipped with a PPT 200 M quadrupole mass spectrometer for residual gas analysis and leak checking. Gas pressures were measured with MKS Baratron capacitance manometers.

2.2. Sample preparation and gas purification

Commercially available alumina (Degussa, 101 m^2/g) was uniformly deposited on a CaF_2 window by spraying a slurry of aluminum oxide suspended in acetone and water (ratio of 9:1). The optical window was placed on a hot plate during spray so that flash evaporation of acetone–water solvent takes place by leaving deposits of the oxide. An appropriate amount of palladium chloride solution was mixed with aluminum oxide slurry for preparing Pd/Al_2O_3 samples and ultrasonically dispersed for approximately 45 min before spraying.

Immediately after spraying, the sample was transferred to the infrared cell and attached to the vacuum manifold overnight for evacuation at ambient temperature. Following evacuation, the sample was slowly heated up to 475 K for 15–20 h. The sample was then reduced using four cycles of 200 Torr H_2 for 15, 30, 45, and 60 min exposures followed by evacuation after each exposure. The sample was evacuated at 475 K for another 12 h followed by cooling to 298 K.

Nitric oxide (99% pure) was obtained in a lecture bottle from Matheson gas. Before the surface is exposed to NO, the gas is passed through an isopentane trap kept at (−160°C) to remove traces of N_2O and NO_2.

3. Results and discussion

3.1. Adsorption of NO on Al_2O_3 and Pd/Al_2O_3

Fig. 1 shows the spectroscopic development due to physical adsorption of NO on reduced aluminum oxide at 110 K. All these spectra were ratioed with a background spectrum collected at the same temperature before adsorption of NO as mentioned in Section 2. Upon adsorption of NO initially three spectral features developed at 1871, 1810, and 1761 cm^{-1} in the ν(N–O) stretching frequency region. The distinct features at 1871 and 1761 cm^{-1} gradually gained intensity (Fig. 1a–g) as a function of increasing NO exposure at 110 K and the band at 1810 cm^{-1} appeared as an unresolved shoulder of the strong 1761 cm^{-1} band. In addition, two weak bands also appeared at 2239 and 1910 cm^{-1}.

Surprisingly several spectral changes in the OH region are observed simultaneously as mentioned. (1) A decrease in intensities of isolated ν(O–H) features at 3730 and 3667 cm^{-1} with concomitant increase in the absorbance of the associated OH stretching frequency (∼3600 cm^{-1}) region occurs. (2) Upon evacuation (not shown in Fig. 1) all ν(N–O) modes disappear and restore the spectral intensities of IR

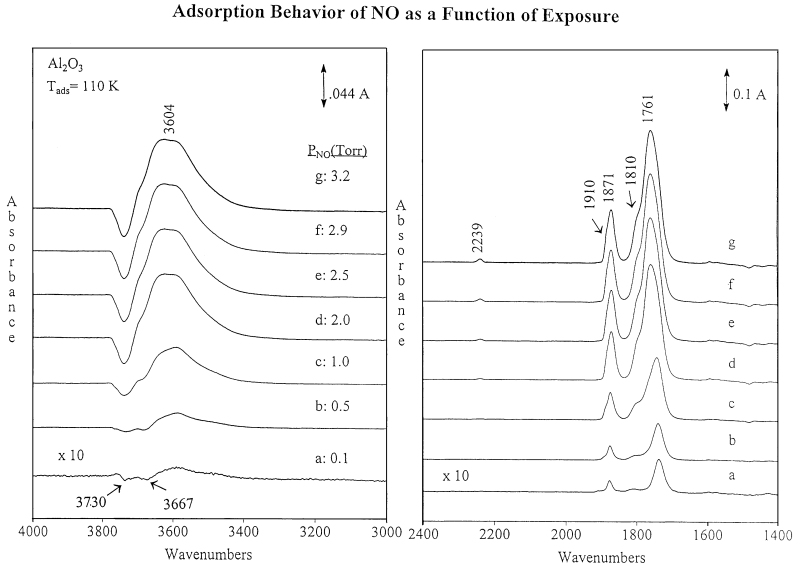

Fig. 1. Infrared spectra in ν(OH) and ν(NO) regions for Al_2O_3 surface for various NO exposures at 110 K.

Table 1
Vibrational (ν_{sym} and ν_{asym}) frequencies (cm^{-1}) for $(NO)_2$ observed in condensed gas phase and matrices

	ν_s(N–O)	ν_{as}(N–O)	References
Gas phase			
cis-$(NO)_2$, 77 K	1860	1788	[27]
Matrix isolated			
N_2 matrix *cis*- and *trans*-$(NO)_2$, 15 K	1870	1776, *trans* 1764	[28]
Argon matrix *cis*-$(NO)_2$	1863.6	1776.2	[29]
Argon matrix *cis*-$(NO)_2$	1866	1776	

features at 3730 and 3670 cm^{-1} while a decrease in the intensity of the associated OH groups is observed.

For assignment purposes, earlier studies of low temperature adsorption of NO are summarized in three tables according to the nature of substrate. Table 1 shows the characterization of *cis*- and *trans*-$(NO)_2$ dimer using IR studies of condensed [27] and matrix isolated NO [28,29]. The structures of these two species are shown below.

cis-(NO_2)dimer *trans*-(NO_2)dimer

The *trans*-$(NO)_2$ has only one absorption peak at ~1764 cm^{-1} [28], whereas the *cis*-$(NO)_2$ isomer has two strong features ν_s and ν_{as} at 1860 and 1776 cm^{-1}, respectively [29]. During low temperature adsorption of NO in the presence of zeolite [14,15] and single crystal metal surfaces [4,6,9–11], $(NO)_2$ formation was characterized by vibrational frequencies at ~1880 and ~1780 cm^{-1} as indicated in Tables 2 and 3. The integrated absorbance ratio of $\int I_{1874}\,d\nu / \int I_{1761}\,d\nu$ remains constant for all NO exposures at 110 K as can be shown (Fig. 2) in a plot of $\int I_{1874}\,d\nu$ versus $\int I_{1761}\,d\nu$. In addition, it is apparent that the decrease in integrated absorbance for the isolated OH groups may be linearly correlated with the increase in integrated absorbance for the antisymmetric ν(N–O) mode.

Table 2
Vibrational (ν_{sym} and ν_{asym}) frequencies (cm^{-1}) for $(NO)_2$ observed on zeolite surfaces[a]

Surfaces	Temperature (K)	ν_s(N–O)	ν_{as}(N–O)
HY zeolite	83	1890	1770
NaY zeolite	83	1880	1775
CaY zeolite	83	1884	1770
HY zeolite	83	1890	1790

[a] [14,15].

Thus, careful judgement of spectral position and shapes for 1871 and 1761 cm^{-1} absorption produced in our present study can be attributed to ν_s(N–O) and ν_{as}(N–O) for $(NO)_2$ adsorbed dimer species. All $(NO)_2$ dimer species as indicated in Table 1 show a combination mode ($\nu_s + \nu_{as}$) at 3600 cm^{-1} [27–29]. Careful investigation of ν(OH) region show that there is an indication of growth of an unresolvable band at

Table 3
Vibrational (ν_{sym} and ν_{asym}) frequencies (cm^{-1}) for $(NO)_2$ observed on single crystal surfaces

Surfaces	Temperature (K)	Dimer formation	ν_s(N–O)	ν_{as}(N–O)	References
Pd(1 1 1)	20	Yes (HREELS)			[4]
Stepped Pd(1 1 1)	160	No			[6]
Pd(1 1 0)	180	No			
Pt(1 1 1)	25–50	Yes (two pairs)	1865	1787	[10]
			1859	1767	
Ag(1 1 1)	70–90	Yes	1863	1788	[12]
	20	Yes (XPS study)			
Ag/Ru(0 0 1)	75	Yes (XPS)			[11]

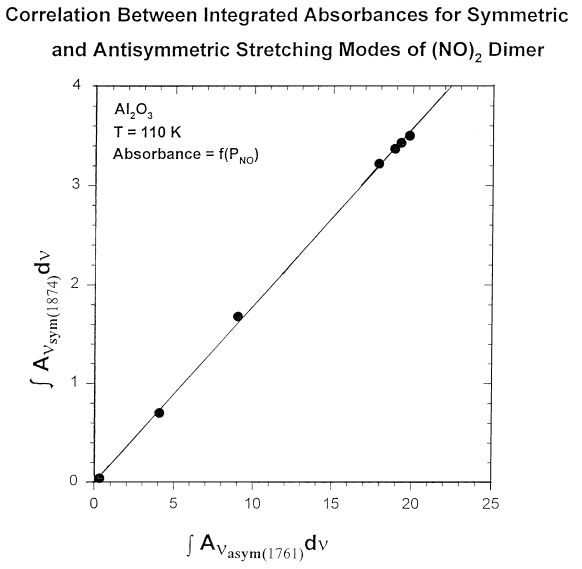

Fig. 2. Integrated absorbance correlation of 1874 cm^{-1} vs. 1761 cm^{-1} peaks which are due to adsorbed NO species on Al_2O_3.

~3600 cm^{-1} along with a broad OH feature for associated –OH groups.

The assignment of non-resolvable small shoulders (at ~1910 and ~1810 cm^{-1}) on the high frequency sides of twin bands of dimers can be signatures of a second pair of dimer. These two pairs of dimers are adsorbed either on different types of sites or the same type of site but with different configurations, and thus the bond lengths and angles of dimer are slightly different.

Recently Yoshinobu and Kawai [10] also identified two $(NO)_2$ dimer species by observation of two symmetric (1865, 1859 cm^{-1}) and two antisymmetric (1787 and 1767 cm^{-1}) stretching vibrations. The 1865 and 1787 cm^{-1} are assigned to the condensed dimer, and 1859 and 1767 cm^{-1} are assigned to the dimer which adsorbs directly on top of the chemisorbed NO species. However, the critical analyses of 1910 and 1810 cm^{-1} were not possible because of overlap with another pair of dimer features. The idea of assigning these two peaks for ν(N–O) for monomeric NO at different sites of Al_2O_3 cannot be ruled out.

Fig. 3 shows the effects of different palladium loading on low temperature NO adsorption over reduced Pd/Al_2O_3. These effects can be observed by investigating spectral changes in the ν(N–O) and ν(O–H) regions. A dramatic decrease in the intensity of the 1874 cm^{-1} band is noticed indicating a decrease in dimer coverage as the Pd loading is increased from 0.5

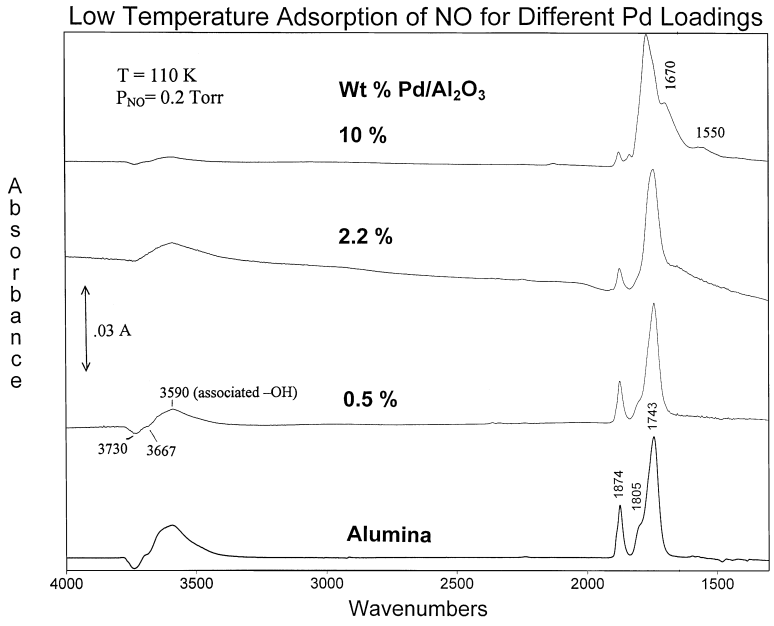

Fig. 3. Infrared spectra in ν(OH) and ν(NO) regions for Al_2O_3 and Pd/Al_2O_3 for various NO exposures at 110 K. Catalyst samples have different Pd loading as mentioned in each spectrum.

to 10%. In addition a significant blue shift ($\sim$30 cm^{-1}) of the 1743 cm^{-1} band indicates a possible site transfer for NO adsorption. Here the NO molecule now adsorbs onto Pd instead of oxide site as Pd loading increases. The newly grown absorption peaks (for 10% Pd loading) at 1670 and 1550 cm^{-1} can be assigned to linear and bridged bound monomeric NO on Pd. These assignments are consistent with the work by Hoost et al. (on Pd/Al_2O_3) [32] and Moriki et al.(on Pd/SiO_2) [33].

The intensities of isolated ν(OH) bands (at 3730 and 3667 cm^{-1}) and associated ν(OH) (at $\sim$3590 cm^{-1}) declined dramatically with an increase in Pd loading indicating that NO adsorption takes place predominantly on Pd instead of alumina sites at higher Pd loadings. As the Pd loading increases, the population of surface –OH groups decreases and fewer NO molecules hydrogen bonds to the surface causing more NO molecules to be bonded to Pd particles.

3.2. Temperature dependence adsorption studies: decomposition of $(NO)_2$ and formation of N_2O

Fig. 4 shows the results of heating the adsorbed NO species. As the cell is gradually warmed above 110 K the intensities of IR features at 1871 and 1761 cm^{-1} started to decrease while the band at 2241 cm^{-1} grows in intensity. The growth of this band continued up to 190 K (spectrum 4d) maintaining its symmetrical narrow peak shape, whereas, at 200 K the peak shape changed to an envelope showing PQR branches (spectrum 4e, 2241 cm^{-1} band) due to overlapping of vibra-

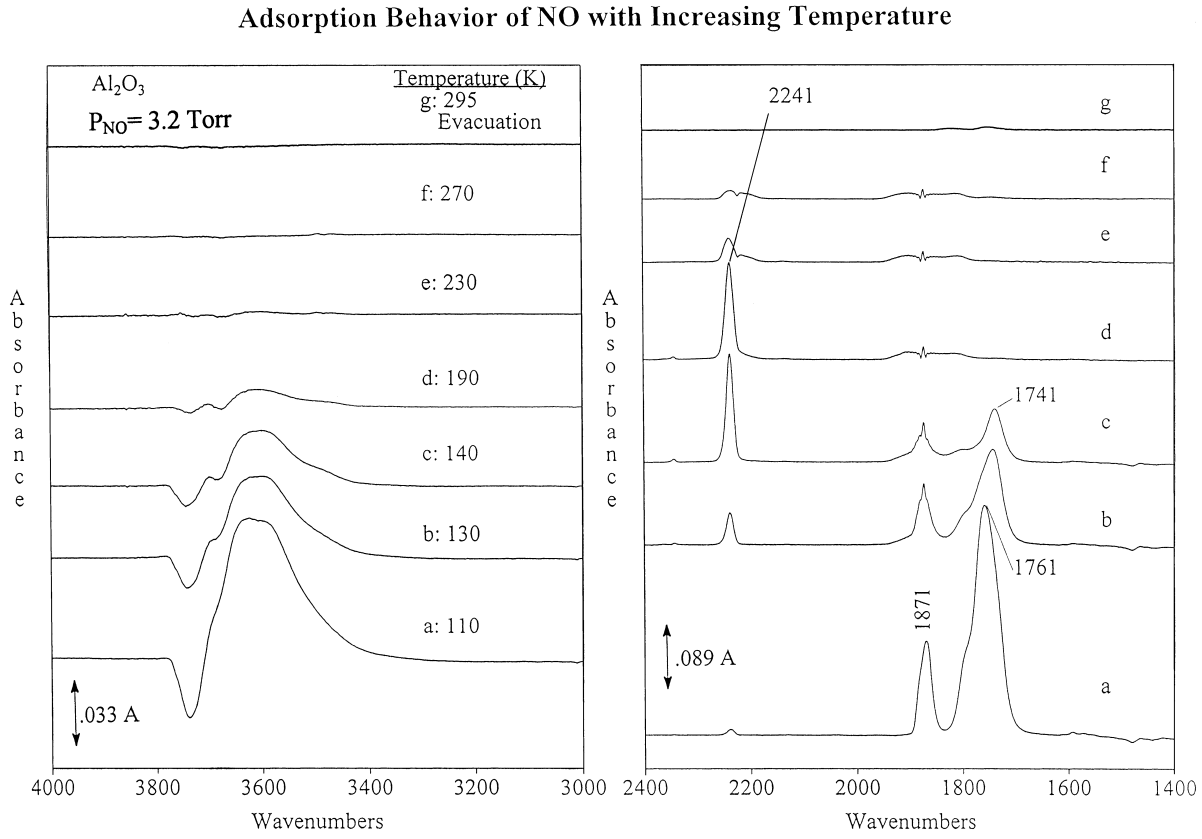

Fig. 4. Infrared spectra in ν(OH) and ν(NO) regions for the reaction NO (adsorbed at 110 K) over an Al_2O_3 surface at different temperatures indicated for each spectrum.

Table 4
Low temperature reactivity of $(NO)_2$ dimer on different surfaces

Surfaces	Products	References
Ag(1 1 1), 63–117 K	N_2O (ad) (2232 cm^{-1})	[12]
Pt(1 1 1)	No reaction	[10]
Pd(1 1 1)	No reaction	[30]
Ag/Ru(0 0 1)	N_2O	[31]
Evaporated Ni (oxidized)	No reaction	[31]
W(1 0 0)	N_2O	[13]
NaY zeolite	N_2O (2240 cm^{-1})	[14,15]
CaY zeolite	N_2O (2250 cm^{-1})	[14,15]
Pd/Al_2O_3	N_2O (2239 cm^{-1})	This work

tional and rotational bands of desorbed gas molecules. Thus the band at 2241 cm^{-1} can be assigned to physisorbed ν(N–N) for N_2O consistent with the assignment made in earlier studies [10,12–15,30,31] as shown in Table 4. As the adsorbed N_2O desorbs from the surface forming N_2O gas, the peak shape changes as discussed. The displayed ratio spectra for ν(OH) regions show the restoration of features at 3740 and 3670 cm^{-1} by decreasing negative intensity. The accompanying intensity decrease of the positive-going feature at ~3650 cm^{-1} is caused by the conversion of associated OH groups to isolated OH groups as the hydrogen bonding (between $(NO)_2$ dimers and isolated OH groups) are broken.

Although a similar NO adsorption behavior is observed for 2.2% Pd/Al_2O_3 at different temperatures in Fig. 5, there is a subtle difference in the NO adsorption behavior as the cell is warmed up to 289 K (compare spectra e, f, and g of Figs. 4 and 5). In Fig. 5, NO adsorption seen at 1764 and 1678 cm^{-1} can be assigned to linear and bridge-bound NO species on Pd.

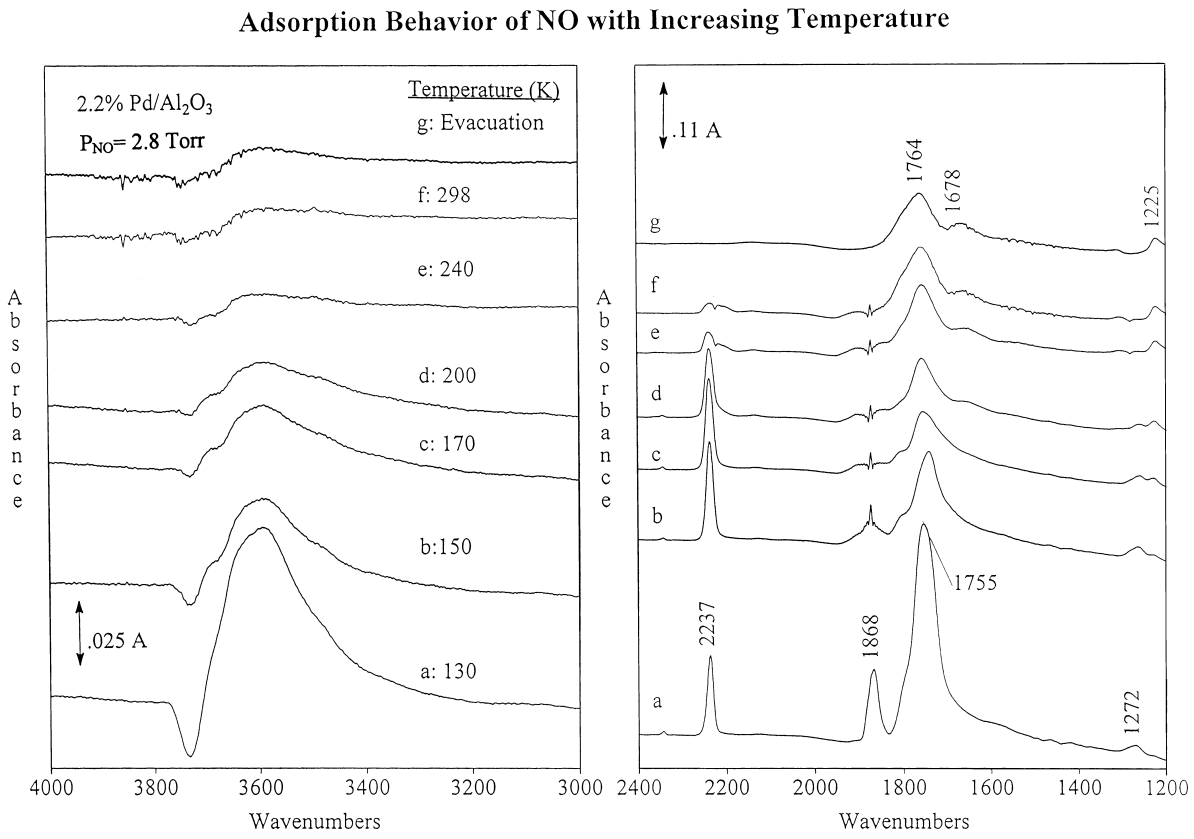

Fig. 5. Infrared spectra in ν(OH) and ν(NO) regions for the reaction NO (adsorbed at 110 K) over a 2.2% Pd/Al_2O_3 film at different temperatures.

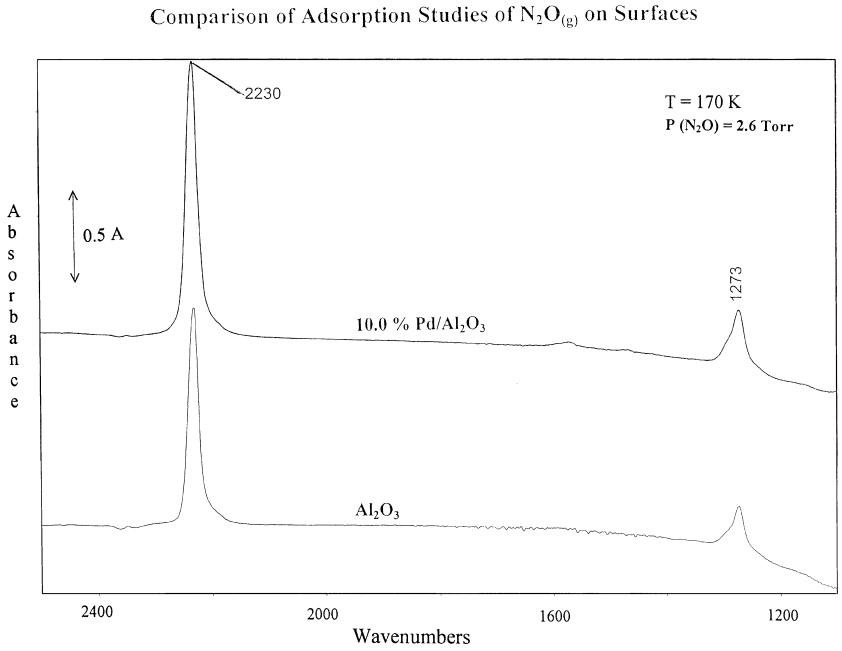

Fig. 6. Infrared spectra for the reaction of N_2O over Al_2O_3 and 10% Pd/Al_2O_3 at 170 K and a pressure of 2.6 Torr.

The proof that the band at 2241 cm^{-1} is due to N_2O formation can be seen in Fig. 6. Here the top and bottom spectra indicate the adsorption of N_2O on 10% Pd/Al_2O_3 and Al_2O_3 at 170 K. The strong band at 2230 for ν(N–N) and the weak band at 1273 cm^{-1} for ν(N–O) indicative for physisorbed N_2O species. This observation is consistent with the specrtrum developed during warm-up of adsorbed NO species, where the ν(N–N) feature developed at 2241 cm^{-1} and the band at 1272 cm^{-1} was very weak and was not shown.

We have therefore shown that NO reacts to form N_2O on Al_2O_3 and Pd/Al_2O_3 at low temperature range of 110–190 K. The possibility cannot be ruled out that some of the NO desorbs, while the rest of it reacts to form N_2O.

3.3. Mechanism of N_2O formation

There are two mechanisms by which N_2O could be formed on the Al_2O_3 surface. The first is via dissociative adsorption of NO:

$$NO \rightarrow N_{ad} + O_{ad}$$

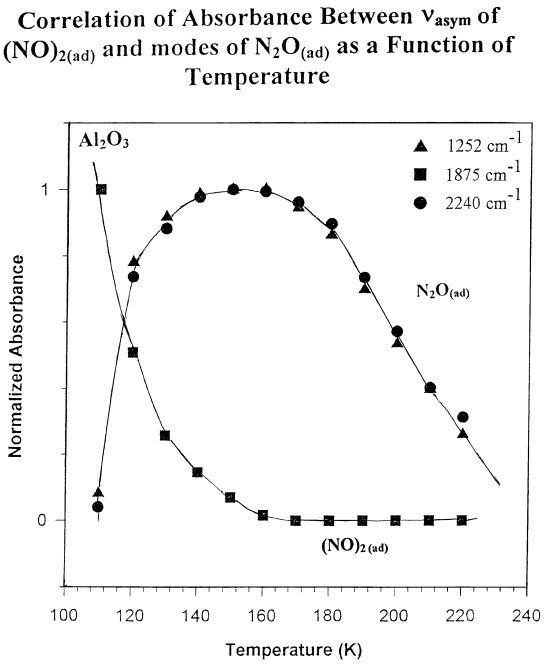

Fig. 7. A plot of the normalized absorbance of the 1875 [ν_{as}(N–O) of $(NO)_2$], 2240 [ν(N–N) of N_2O] and 1252 cm^{-1} [ν(N–O) of N_2O] bands observed on Al_2O_3 vs. temperature.

$NO_{ad} + N_{ad} \rightarrow N_2O_{ad}$

The second mechanism is via the formation of $(NO)_2$ dimers:

$2NO + (NO)_{2ad} \rightarrow N_2O_{ad} + O_{ad}$

The observation of the $(NO)_2$ dimer on the surface at all coverages provides strong support for the second mechanism. Further support for this mechanism is provided by the plot shown in Fig. 7. The figure shown a plot of the amount of $(NO)_2$ and N_2O on the surface versus temperature, as determined by integrating the areas under the 1875 cm^{-1} [$(NO)_2$] and the 2240 and 1250 cm^{-1} [N_2O] infrared bands that were observed when adsorbed NO was heated. Since the band frequencies are independent of NO coverage, the assumption of proportionality between integrated absorbance and the amount of adsorbed species can be made. The absorbance was then normalized so that the maximum peak intensity was equal to an absorbance of unity.

As can be seen in Fig. 7, the N_2O bands grow in as the $(NO)_2$ band decreases, and in fact the curves are almost mirror images of each other as also observed by Brown et al. [12]. This shows the evidence that the $(NO)_2$ reacts directly to form N_2O. This pathway for N_2O formation is favored by Brown et al. [12] on Ag(1 1 1) and Friend et al. [13] on W(1 0 0) surfaces. Cho and Lunsford [14,15] suggested that the observation of N_2O formation on NaY and CaY-zeoltes may result from the dissociation of dimers adsorbed on positive charged sites of Na^+ or Ca^{2+}.

The following experiments also do not favor the formation of N_2O via disscoiative adsorption of NO. The first experiment involves the NO/CO coadsorption

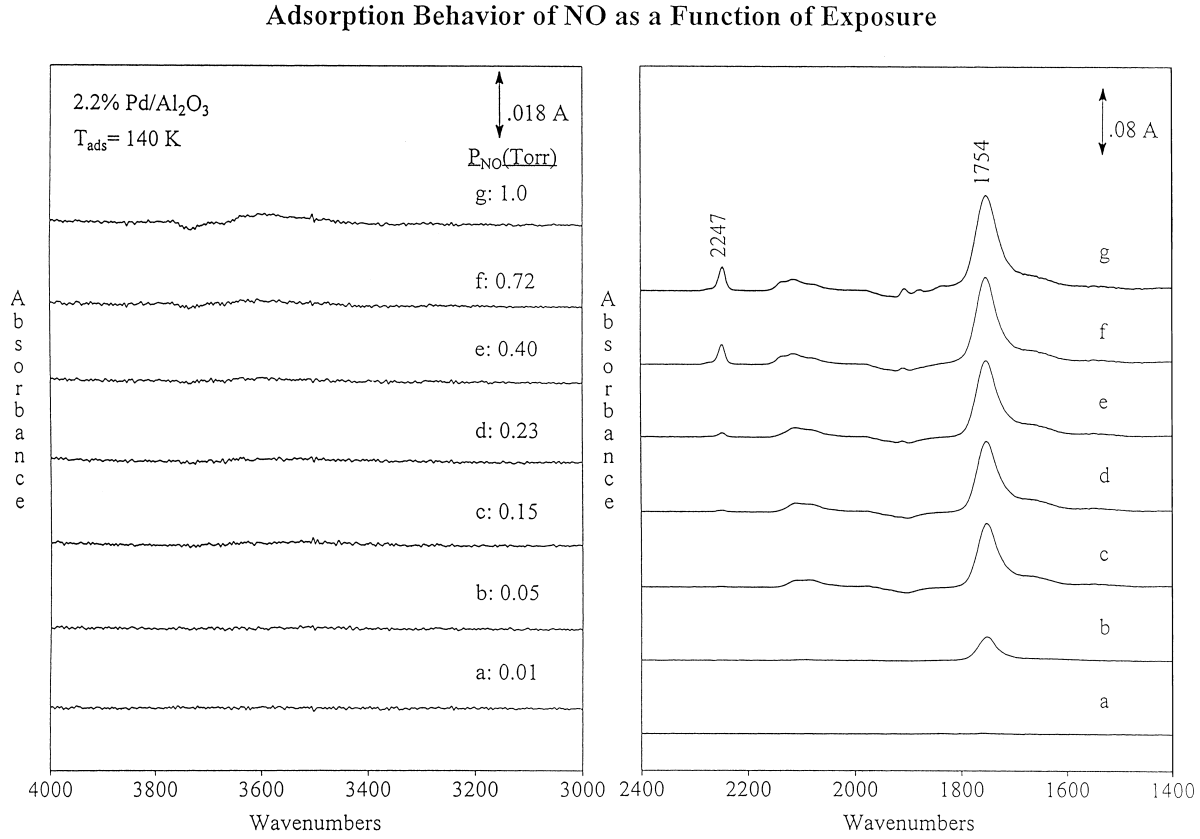

Fig. 8. Infrared spectra in ν(OH) and ν(NO) regions for 2.2% Pd/Al_2O_3 for various NO exposures at 140 K.

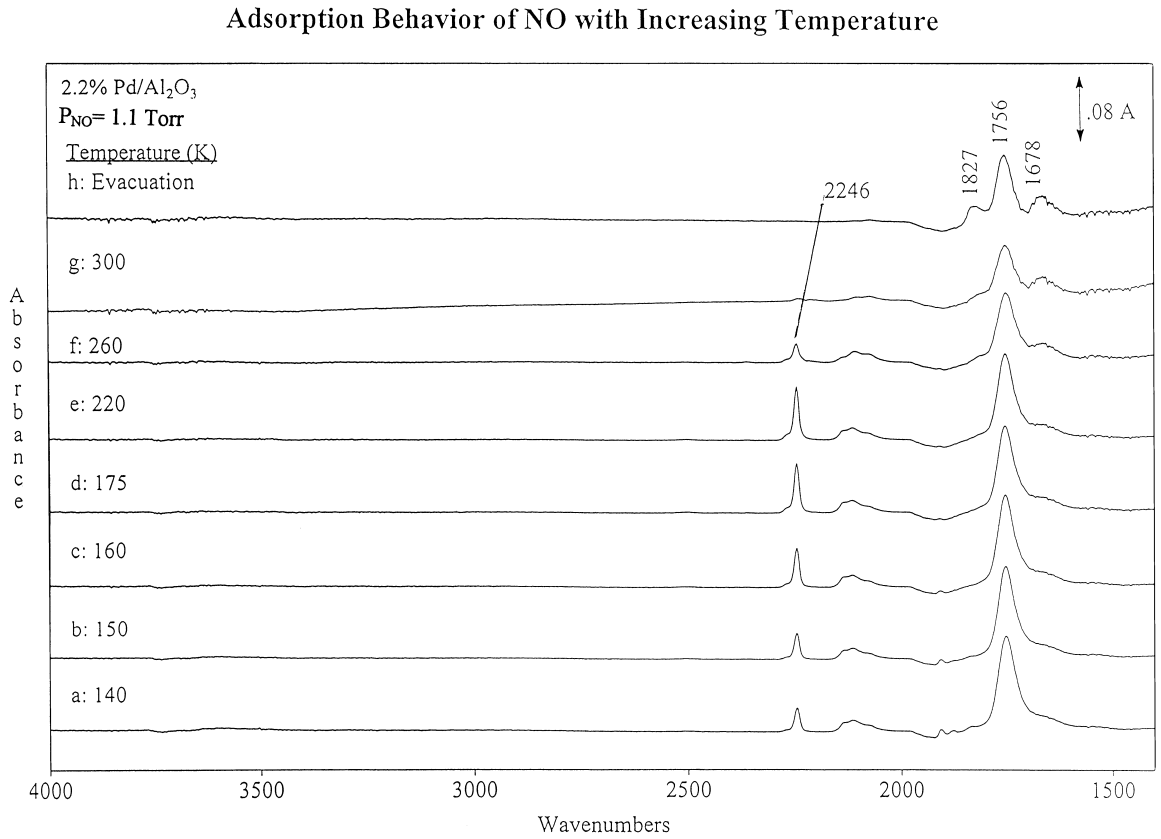

Fig. 9. Infrared spectra for 2.2% Pd/Al_2O_3 for the reaction of NO (adsorbed at 140 K) at different temperatures indicated as the sample is warmed up.

(at 110–300 K) did not produce any detectable isocyanate (–NCO) species on the surface (see detail in Section 3.5). In the second experiment CO was adsorbed onto a surface on which NO was previously adsorbed prior to heating the surface to 200 K to desorb any gas phase NO and N_2O leaving behind any dissociated N and O atoms. Adsorption of CO at different temperatures did not indicate any bands due to isocyanate surface species.

3.4. Influence of adsorption temperature on dimer formation

Fig. 8 shows the adsorption behavior of NO at 140 K over 2.2% Pd/Al_2O_3 with increase in NO pressure. Here the infrared feature at 1754 cm^{-1} gradually intensifies as a function of NO coverage. This can be assigned ν(NO) for linear adsorption of NO.

Investigation of the ν(OH) region indicates, there is no change in spectral intensities for ν(OH) peaks. Since only one adsorption peak is predominantly present in the ν(N–O) stretching region, and the dimer formation is characterized by twin peaks for ν_s(NO) and ν_{as}(NO), there is a lack of dimer formation on this surface at 140 K. Thus, adsorption temperature play an active role in dimer formation.

The spectral changes observed upon warming the cell from 140 to 298 K are shown Fig. 9. Here the production of 2246 cm^{-1} (N_2O species) was insignificant compared to the spectrum taken for 110 K adsorption. The other new bands developed at 1827 and

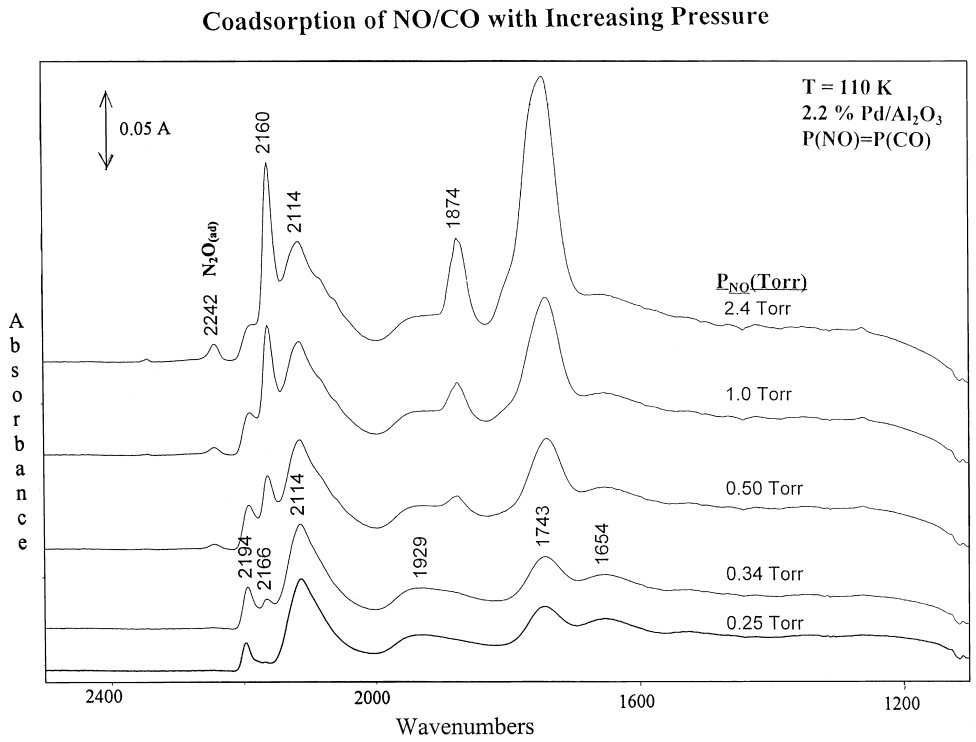

Fig. 10. Infrared spectra for NO and CO coadsorption over a 2.2% Pd/Al_2O_3 film for various exposures at 110 K.

1678 cm^{-1} are due to activated chemisorption of NO on Pd metal surfaces.

3.5. Search for isocyanate (–NCO) formation

Fig. 10 shows the spectral development due to coadsorption of NO and CO at 110 K over 2.2% Pd/Al_2O_3. The bands developed can be grouped into two regions: the ν(CO) region has bands at 2194, 2166, 2114, and 1929 cm^{-1} and the ν(NO) region has two bands at 1743 and 1654 cm^{-1}. The band at 2194 cm^{-1} can be assigned to ν(CO) bonded to Lewis acid site (Al^{3+}) and the band at 2166 cm^{-1} is hydrogen bonded to Al–OH groups. These assignments are consistent with the studies by Yates and coworkers [34,35]. The low frequency modes for CO absorption (2114 and 1874 cm^{-1}) are due to linearly and bridge bound CO on palladium metal [36]. The ν(NO) modes at 1874 and 1743 cm^{-1} are due to the $(NO)_2$ dimer and a fraction of molecules are linearly bound ON–Pd^0.

As the coadsorbent gas pressure is increased the intensities of both NO and CO stretching modes gradually increase indicating that NO and CO coadsorbed on different sites. As the surface is gradually warmed up (Fig. 11) the formation of N_2O is observed at 2241 cm^{-1} and the strong IR features at 2192 and 2163 cm^{-1} due to ν(CO) gradually disappear indicating that these bonds are weak [34,35]. Ultimately after warming up to room temperature, both chemisorbed CO and NO peaks are clearly noticeable.

Two types of isocyanates have been identified earlier on alumina-supported metal surfaces [36–39]. Aluminium oxide bound isocyanate (2246 cm^{-1}) is stable up to 400 K and upon evacuation, whereas Pd-bound isocyanate (2180 cm^{-1}) is not stable and migrates to the support site [36–39]. The isocyanate formation is possible from this reaction if NO disscociates at 110 K, however, since the coadsorption of NO and CO at different temperatures does not show any spectroscopic evidence for –NCO formation, we

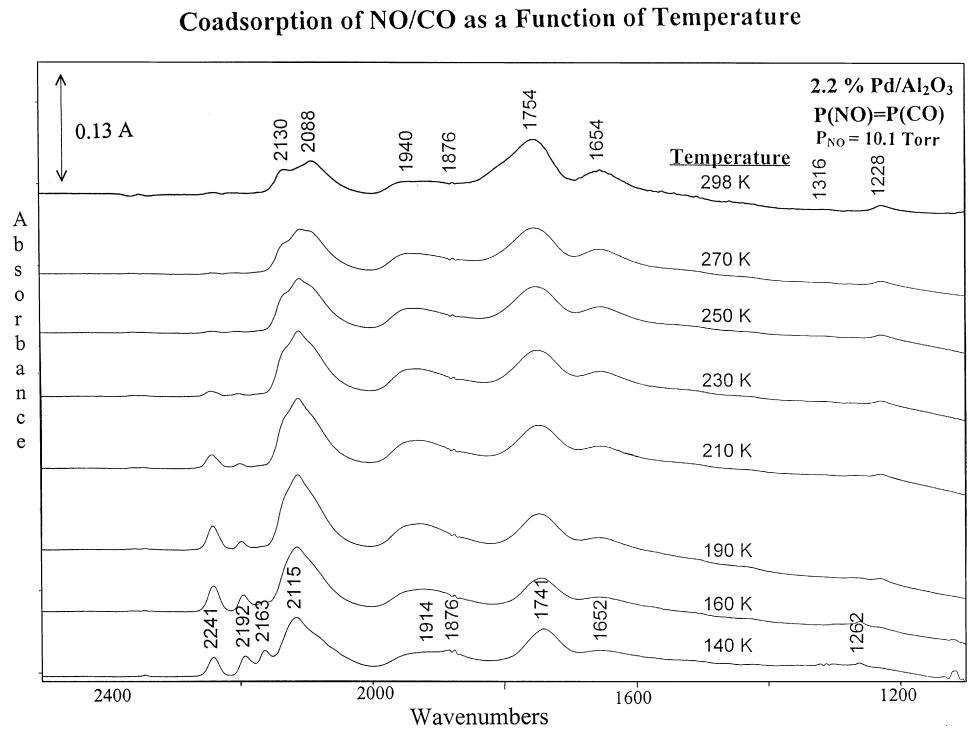

Fig. 11. Infrared spectra for the reaction of NO and CO over a 2.2% Pd/Al_2O_3 film at various temperatures as indicated in each spectrum.

believe the NO dissociation mechanism is not favored at this low temperature.

4. Conclusions

On the basis of the discussion presented above, the following conclusions are drawn regarding NO adsorption and decomposition on both Al_2O_3 and Pd/Al_2O_3.

NO adsorbs molecularly at 110 K on isolated hydroxyl groups via hydrogen bonding. Only isolated OH groups on the Al_2O_3 surface are involved in the adsorption as judged by the spectral changes occurring in the characteristic ν(O–H) features.

The $(NO)_2$ dimers have been seen at 110 K and are stabilized by surface –OH groups. Recent infrared data indicate that functionalization [40] of –OH groups using chlorotrimethyl silane can be used to prevent stablization of the dimer. Formation of N_2O results from adsorbed $(NO)_2$ dimer instead of dissociation of the N–O bond at low temperature. No isocyanate (–NCO) formation was detected upon coadsorption of NO/CO at different temperatures.

Acknowledgements

We thank the Research Corporation for the support of this work. We wish to acknowledge with pleasure the useful discussions with Sister Mary O'Rourke, Ph.D., Department of Chemistry, Rockhurst University.

References

[1] R.J. Farrauto, R.M. Heck, B.K. Speronello, Chem. Eng. News 34 7 September (1992).
[2] G. Busca, L. Lietti, G. Ramis, F. Berti, Appl. Catal. B 18 (1998) 1.
[3] K. Hashimoto, K. Fukuhara, Y. Fujiwara, H. Kominami, H. Mishiima, Y. Kera, Appl. Catal.: Gen. 165 (1997) 451.
[4] M. Bertolo, K. Jacobi, Surf. Sci. 226 (1990) 207.

[5] M. Bertolo, K. Jacobi, S. Nettesheim, M. Wolf, E. Hasselbrink, Vacuum 41 (1990) 76.
[6] H.-D. Schmick, H.W. Wassmuth, Surf. Sci. 123 (1982) 471.
[7] P.J. Chen, D.W. Goodman, Surf. Sci. 297 (1993) L93.
[8] W. Ranke, Surf. Sci. 209 (1989) 57.
[9] H. Ibach, S. Lehald, Surf. Sci. 76 (1978) 1.
[10] J. Yoshinobu, M. Kawai, Chem. Lett. (1995) 605.
[11] C. Ludviksson, C. Huang, H.J. Jansch, R.M. Martin, Surf. Sci. 284 (1993) 328.
[12] W.A. Brown, P. Gardner, D.A. King, J. Phys. Chem. 99 (1995) 7065.
[13] E.K. Baldwin, C.M. Friend, J. Phys. Chem. 89 (1985) 2576.
[14] C.-C. Cho, J.H. Lunsford, J. Am. Chem. Soc. 93 (1971) 71.
[15] C.-C. Cho, J.H. Lunsford, J. Am. Chem. Soc. 93 (1971) 25.
[16] M.-C. Wu, D.W. Goodman, J. Phys. Chem. 98 (1994) 9874.
[17] C.N. Rusu, J.T. Yates Jr., J. Phys. Chem. B 104 (2000) 1729.
[18] J.B. Peri, R.B. Hannan, J. Phys. Chem. 64 (1960) 1526.
[19] J.B. Peri, J. Phys. Chem. 69 (1965) 220.
[20] J.B. Peri, J. Phys. Chem. 64 (1960) 1526.
[21] H. Knozinger, P. Ratnasamy, Catal. Rev.-Sci. Eng. 17 (1) (1978) 31.
[22] E.B. Cornelius, T.H. Mullikan, G.A. Mills, A.G. Oblad, J. Phys. Chem. 59 (1955) 809.
[23] A.V. Kiselev, V.I. Lygin, Infrared Spectra of Surface Compounds, Wliey, New York, 1975.
[24] M.L. Hair, Infrared Spectroscopy in Surface Chemistry, Marcel Dekker, New York, 1967.
[25] L.H. Little, Infrared Spectra of Adsorbed Species, Academic Press, New York, 1966.
[26] T.P. Beebe, P. Gelin, J.T. Yates Jr., Surf. Sci. 148 (1984) 526.
[27] C.E. Dinerman, G.E. Ewing, J. Chem. Phys. 53 (1970) 626.
[28] W.A. Guillory, C.E. Hunter, J. Chem. Phys. 50 (1969) 3516.
[29] J.F. Canty, E.G. Stone, S.B. Bach, D.W. Ball, Chem. Phys. 216 (1997) 81.
[30] W.G. Fately, H.A. Bent, B. Crawford Jr., J. Chem. Phys. 31 (1959) 204.
[31] D.T. Wickham, B.A. Banse, B.E. Koel, Surf. Sci. 243 (1991) 83.
[32] T.E. Hoost, K. Otto, K.A. Laframboise, J. Catal. 155 (1995) 303.
[33] S. Moriki, Y. Inoue, E. Miyazaki, I. Yasumori, J. Chem. Soc., Faraday Trans. 1 78 (1982) 171.
[34] H.P. Wang, J.T. Yates Jr., J. Catal. 89 (1984) 79.
[35] T.H. Ballinger, J.T. Yates Jr., Langmuir 7 (1991) 3041.
[36] D.K. Paul, S.D. Worley, J. Phys. Chem. 94 (1990) 8956.
[37] D.K. Paul, S.D. Worley, N.W. Hoffman, D.H. Ash, J. Gautney, Surf. Sci. 223 (1989) 509.
[38] D.K. Paul, S.D. Worley, N.W. Hoffman, D.H. Ash, J. Gautney, Chem. Phys. Lett. 160 (1989) 559.
[39] D.K. Paul, C.D. Marten, Langmuir 14 (1998) 3820.
[40] D.K. Paul, A. Jaber, in preparation.